

## Notes

### Phase-Transition Thermodynamics of *N*-Isopropylacrylamide Hydrogels

Charles V. Rice\*

Department of Chemistry and Biochemistry, University of Oklahoma, 620 Parrington Oval, Room 208, Norman, Oklahoma 73019

Received June 26, 2006

Many polymer solutions exhibit a lower critical-solution temperature (LCST), above which the polymer is insoluble. The transition from a homogeneous mixture to phase separation is abrupt, within 1–2 °C, and has fascinated researchers for decades. Interest lies not only in an attempt to understand the fundamental chemical mechanism but also to harness LCST behavior in various applications. Currently, many laboratories are exploring temperature-sensitive polymers for drug delivery<sup>1–4</sup> and tissue scaffolds.<sup>3,5–9</sup>

Molecular-level engineering strategies, such as the addition of copolymers,<sup>10–15</sup> are used to control the phase-separation process and to tailor the LCST for specific needs. The primary analytical tools are cloud-point measurements<sup>16,17</sup> (to determine LCST) and differential scanning calorimetry, whose enthalpy measurements are used to support phase-transition mechanisms.<sup>16,18</sup> These data provide an incomplete picture. Cloud points are not quantitative and the  $\Delta H_{DSC}$  may not correlate with the van't Hoff  $\Delta H^\circ$ , expressed by the “cooperative unit”.<sup>19,20</sup> Entropic factors should play a major role in polymer precipitation, yet values for  $\Delta S^\circ$  remain a mystery. The need for quantitative data within “orders of magnitude” has been suggested.<sup>21</sup> Using NMR spectroscopy, we have determined  $\Delta H^\circ$ ,  $\Delta S^\circ$ , and  $\Delta G^\circ$  for an *N*-isopropylacrylamide (NiPAAm) hydrogel. These data present a picture of the phase-transition process. This fundamental chemical information will allow researchers to understand how additives, such as copolymers or pharmaceuticals, affect the enthalpic and entropic processes.

*N*-Isopropylacrylamide (NiPAAm) is widely studied due to its LCST near ambient temperatures.<sup>16,22</sup> The current LCST mechanism for NiPAAm/water solutions involves the loss of water solvent in the hydration sphere and exposure of the hydrophobic backbone to the solvent, which results in a loss of water solubility. Measurements from differential scanning calorimetry report enthalpy changes of 4–7 kJ/(mol repeat unit),<sup>1,23</sup> which are assigned to the loss of water hydrogen bonds to the carbonyl and amine groups. Yet, water hydrogen bonds have a  $\Delta H^\circ \sim 12$  kJ/mol,<sup>24</sup> and recent IR studies suggest minimal change to the carbonyl and amine chemical environment.<sup>23</sup> Since the polymer structure is believed to go through a coil-to-globule transition, the change in entropy should be significant. An influential review article by Schild<sup>16</sup> (cited nearly 800 times) suggests that, qualitatively,  $\Delta S^\circ$  is negative.

With variable-temperature NMR data of the NiPAAm phase-transition process, we have determined  $\Delta H^\circ$  to be endothermic and  $\Delta S^\circ$  to be positive, which yields a positive  $\Delta G^\circ$  for

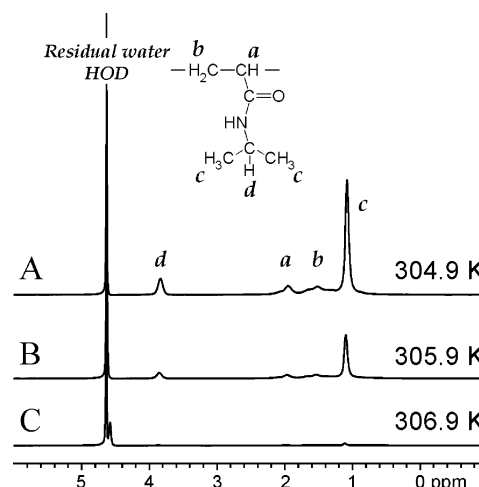


**Figure 1.** Variable-temperature  $^1\text{H}$  HRMAS NMR data of 300:1 poly-(NiPAAm). The loss of signal intensity is caused by the phase transition into a solid polymer, which cannot be observed. Thus, the remaining signal represents the flexible portion and provides quantitative information regarding the phase transition.

precipitation at room temperature. These data suggest that the phase transition begins with the loss of interactions between polymer hydrophobic segments.

Hydrogels of *N*-isopropylacrylamide were formed by cross-linking with BIS at a ratio of 300:1 (NiPAAm:BIS) using photopolymerization. NMR data were collected using a high-resolution magic-angle spinning (HRMAS), whose deuterium lock channel provides the ability to correct (via shimming) temperature-induced changes in chemical shift and field inhomogeneities within the sample, factors that affect the natural line width.<sup>28–30</sup> The HRMAS sample rotor also restricts the sample to the probe coil region such that the NMR data represent the entire sample and polymer precipitation does not affect our quantitative analysis.

During the phase transition, the sample is a heterogeneous mixture of collapsed and swollen hydrogel domains, creating differences in magnetic susceptibility and significant line broadening. Fortunately, MAS removes magnetic susceptibility effects and allows us to collect high-resolution data for the swollen hydrogel fraction. Reduced molecular motion in the collapsed material creates severe line broadening from CSA and dipole–dipole coupling effects. Additional solid-state NMR methods, including very high radio frequency (rf) power and two-dimensional pulse sequences, are needed to collect well-resolved  $^1\text{H}$  NMR spectra.<sup>25–27</sup> Our HRMAS probe cannot deliver the high rf power necessary to observe the collapsed fraction in the NMR spectra. Thus, HRMAS NMR data represent flexible portions of the hydrogel, and signal loss during the phase transition (Figure 1) is used to quantify the amount of flexible domains within the sample.

The  $^1\text{H}$  NMR peak intensity for the methyl groups (peak c) is plotted in Figure 2 as a function of temperature. Normalization with respect to the tallest signal (which occurs at 302 K) permits a quantitative assessment of the phase transition. The plot of

\* E-mail: rice@ou.edu.

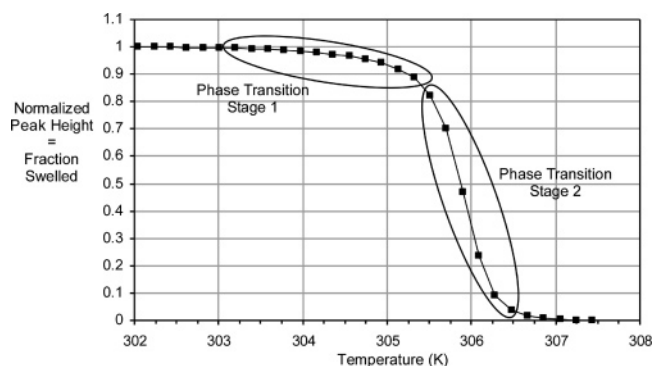


**Figure 2.** Plot of methyl group intensity (peak c, Figure 1) as a function of temperature. It is clear that the first stage of the phase transition (between 302 and 305.5 K) is gradual, while the second stage (305.5–307 K) is quite rapid. Signal intensities below 302 K were unity, while NiPAAm signals above 307 K were miniscule.

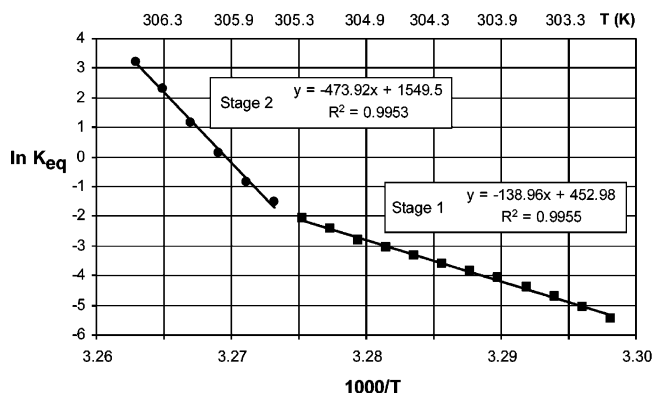


**Figure 3.** The equilibrium constant was found from the fraction of collapsed/swelled, determined from Figure 2. The van't Hoff plot clearly shows a two-stage process, which have very different enthalpic and entropic components. Stage 1 is shown by filled squares, while filled circles represent stage 2. The  $\Delta H^\circ$  and  $\Delta S^\circ$  from the slope and intercept were divided by 300 to obtain these parameters in the units of kJ/(mol monomer).  $\Delta H^\circ(1) = 3851 \pm 3$  J/mol,  $\Delta H^\circ(2) = 13134 \pm 16$  J/mol,  $\Delta S^\circ(1) = 12.55 \pm 0.9$  J/(mol K), and  $\Delta S^\circ(2) = 42.94 \pm 0.5$  J/(mol K).

signal intensity vs temperature can be described by three regions. The first, below 305.2 K, shows a slight loss of signal ( $\sim 10\%$ ) as polymer aggregation begins. We do not believe that the signal decrease is due to a change in dynamics, as the line width remains unchanged. Above 305.2 K, the loss of signal is dramatic as the polymer continues the phase transition. Signals above 307 K could not be observed due to significant dipolar and CSA broadening in the collapsed (rigid) polymer network.

The phase transition is an equilibrium process of the competing swelled and collapsed states, governed by the Gibbs free energy for precipitation ( $\Delta G^\circ$ ). The equilibrium constant,  $K_{eq}$ , which is equal to the ratio [collapsed]/[swelled], can be determined by from the NMR data in Figure 1. In this case,  $K_{eq} = ([total] - [swelled])/[swelled]$ , where [total] is determined from the NMR peak intensity at 302 K, well below the LCST. The plot in Figure 2 suggests a two-step process, where modest aggregation (up to 305.2 K) is followed by a dramatic shift to the collapsed state (305–307 K). A van't Hoff plot (Figure 3) verifies this observation.

The enthalpy of precipitation for stage 1 ( $3.851 \pm 0.003$  kJ/mol) is endothermic. Stage 2 is also endothermic, and  $\Delta H^\circ = 13.134 \pm 0.016$  kJ/mol. The van't Hoff  $\Delta S^\circ$  is  $12.55 \pm 0.9$  J mol $^{-1}$  K $^{-1}$  for stage 1 and  $42.94 \pm 0.5$  J mol $^{-1}$  K $^{-1}$  for stage 2. These values allow the calculation of  $\Delta G^\circ$ , 0.108 kJ mol $^{-1}$  and 0.331 kJ mol $^{-1}$  for stages 1 and 2, respectively.

Very small values of  $\Delta G^\circ$  have been observed;<sup>17</sup> therefore, at room temperature, NiPAAm is quite close to LCST ( $\Delta G^\circ = 0$ ). Below LCST, the polymer adopts a coil structure stabilized by a hydration sphere. Upon heating, coil rearrangement begins, exposing hydrophobic portions to the water.  $\Delta H^\circ$  for stage 1 is on the order of hydrophobic bond dissociation energies.<sup>24,31</sup> Collapse of the polymer network occurs when the hydration shell is disrupted, during which the polymer converts to a globule form. Stage 2 is also endothermic, and  $\Delta H^\circ = 13.1$  kJ/mol, comparable to water hydrogen-bond enthalpies. Our data reflect enthalpy per monomer repeat unit; thus, NiPAAm hydration includes, on average, a single hydrogen bond to the water, which could be to the carbonyl, amine, or a combination of both.

Modest rearrangement in stage 1 is also supported by the entropic factors. Breaking hydrogen bonds in stage 2 would greatly increase disorder, which shows a larger increase in entropy. This value is positive not only from the release of water, but the globule represents a state of higher entropy, as the there are many different ways the polymer can fold, increasing configurational entropy.<sup>20,21</sup>

A two-step process has been suggested previously from cloud-point data,<sup>14</sup> and a recent report suggests that one stage is governed by hydrophobic interactions while the other is dominated by amide–water bonds.<sup>32</sup> These important chemical insights can now be envisioned from a thermodynamic viewpoint formulated from our NMR data.

**Acknowledgment.** This work is supported by The University of Oklahoma and a CAREER Award from the National Science Foundation (CHE-0449622).

**Supporting Information Available.** Hydrogel photopolymerization procedures and NMR data collection. This material is available free of charge via the Internet at <http://pubs.acs.org>

## References and Notes

- Gan, D. J.; Lyon, L. A. *J. Am. Chem. Soc.* **2001**, *123* (31), 7511–7517.
- Hoffman, A. S. *Adv. Drug Delivery Rev.* **2002**, *54* (1), 3–12.
- Peppas, N. A.; Huang, Y.; Torres-Lugo, M.; Ward, J. H.; Zhang, J. *Annu. Rev. Biomed. Eng.* **2000**, *2*, 9–29.
- Mori, T.; Maeda, M. *Langmuir* **2004**, *20* (2), 313–319.
- Yong Lee, K.; Mooney, D. J. *Chem. Rev.* **2001**, *101*, 1869–1879.
- Schmidt, C. E.; Leach, J. B. *Annu. Rev. Biomed. Eng.* **2003**, *5*, 293–347.
- Vogel, V.; Baneyx, G. *Annu. Rev. Biomed. Eng.* **2003**, *5*, 441–463.
- Griffith, L. G.; Naughton, G. *Science* **2002**, *295*, 1009–1014.
- Hench, L. L.; Polak, J. M. *Science* **2002**, *295*, 1014–1017.
- Okamura, H.; Morihara, Y.; Masuda, S.; Minagawa, K.; Mori, T.; Tanaka, M. *J. Polym. Sci., Part A: Polym. Chem.* **2002**, *40* (12), 1945–1951.
- Motokawa, R.; Morishita, K.; Koizumi, S.; Nakahira, T.; Annaka, M. *Macromolecules* **2005**, *38* (13), 5748–5760.
- Feil, H.; Bae, Y. H.; Jan, F. J.; Kim, S. W. *Macromolecules* **1993**, *26* (10), 2496–2500.
- Cai, W. S.; Gan, L. H.; Tam, K. C. *Colloid Polym. Sci.* **2001**, *279* (8), 793–799.
- Qiu, X. P.; Kwan, C. M. S.; Wu, C. *Macromolecules* **1997**, *30* (20), 6090–6094.
- Percot, A.; Zhu, X. X.; Lafleur, M. *J. Polym. Sci., Polym. Phys.* **2000**, *38* (7), 907–915.
- Schild, H. G. *Prog. Polym. Sci.* **1992**, *17* (2), 163–249.
- Freitag, R.; Garret-Flaudy, F. *Langmuir* **2002**, *18* (9), 3434–3440.
- Schild, H. G.; Tirrell, D. A. *J. Phys. Chem.* **1990**, *94* (10), 4352–4356.
- Shan, J.; Chen, J.; Nuopponen, M.; Tenhu, H. *Langmuir* **2004**, *20* (11), 4671–4676.
- Robertson, A. D.; Murphy, K. P. *Chem. Rev.* **1997**, *97* (5), 1251–1267.

- (21) Bruscolini, P.; Buzano, C.; Pelizzola, A.; Pretti, M. *Macromol. Symp.* **2002**, 181, 261–273.
- (22) Kubota, K.; Fujishige, S.; Ando, I. *J. Phys. Chem.* **1990**, 94 (12), 5154–5158.
- (23) Maeda, Y.; Nakamura, T.; Ikeda, I. *Macromolecules* **2001**, 34 (5), 1391–1399.
- (24) Laidler, K. J.; Meiser, J. H.; Sanctuary, B. C. *Physical Chemistry*, 4th ed.; Houghton Mifflin: Boston, 2003; p xvi, 1060 p.
- (25) Diez-Pena, E.; Quijada-Garrido, I.; Barrales-Rienda, J. M.; Schnell, I.; Spiess, H. W. *Macromol. Chem. Phys.* **2004**, 205 (4), 438–447.
- (26) Diez-Pena, E.; Quijada-Garrido, I.; Barrales-Rienda, J. M.; Schnell, I.; Spiess, H. W. *Macromol. Chem. Phys.* **2004**, 205 (4), 430–437.
- (27) Diez-Pena, E.; Quijada-Garrido, I.; Barrales-Rienda, J. M.; Wilhelm, M.; Spiess, H. W. *Macromol. Chem. Phys.* **2002**, 203 (3), 491–502.
- (28) Piotto, M.; Elbayed, K.; Wieruszkeski, J. M.; Lippens, G. *J. Magn. Reson.* **2005**, 173 (1), 84–89.
- (29) Hoffman, R. E.; Becker, E. D. *J. Magn. Reson.* **2005**, 176 (1), 87–98.
- (30) Doty, F. D.; Entzminger, G.; Yang, Y. A. *Concept Magn. Res.* **1998**, 10 (4), 239–260.
- (31) Ben-Naim, A. *Hydrophobic Interactions*; Plenum Press: New York, 1980; p 205.
- (32) Zhang, Y. J.; Furryk, S.; Bergbreiter, D. E.; Cremer, P. S. *J. Am. Chem. Soc.* **2005**, 127 (41), 14505–14510.

BM060607T